A 1.4-GHz Radiometer for Internal Body Temperature Measurements

1 AUTHOR:

Parisa Momenroodaki
University of Colorado Boulder

12 PUBLICATIONS   **5** CITATIONS

SEE PROFILE

A 1.4-GHz Radiometer for Internal Body Temperature Measurements

Parisa Momenroodaki, Zoya Popovic
Department of Electrical, Computer and Energy Engineering
University of Colorado at Boulder, Boulder, Colorado, USA
Parisa.Momenroodaki@colorado.edu
Zoya.Popovic@colorado.edu

Robert Scheeler
First RF Corporation
Boulder, Colorado, USA
Robert.Scheeler@colorado.edu

Abstract—**This paper presents a 1.4-GHz microwave radiometer for noninvasive measurements of internal (core) body temperature. The 1.4GHz frequency of operation is chosen for deep cm-range penetration into tissues, as well as low radio-frequency interference (RFI). The radiometer is implemented with off-the-shelf components with several near-field probes. System measurements and temperature estimation are compared for a dipole and circular patch probe, with about 0.5K temperature sensitivity on a single-layer water phantom. These results show a path to a wearable thermometer for sub-surface body temperature measurements.**

Keywords—Radiometry, core body temperature, passive measurements, black-body radiation, detector, biological tissues.

I. INTRODUCTION

There are a number of health-related applications which benefit from the knowledge of internal (core) body temperature. Generally, the external temperature differs from the temperature of internal tissues inside a human body by as much as 2.5K, and also varies during the day [1]. In a number of disorders, this temperature difference varies from that in a healthy body. For example, long duration of exercise, such as in the case of athletes or soldiers under heavy training, can provoke brain heating leading to premature fatigue and even death. Cancer cells can have increased temperatures, as can inflamed tissues such as joints of arthritis patients. Sleeping disorders are accompanied by changes in the circadian cycle, which are in turn related to changes in phase and amplitude of periodic core body temperature variations [2]. Infants suffering from hypoxia-ischemia have an elevated brain temperature, and if detected can be effectively treated [3]. In addition to diagnostics, therapy can be assisted by internal temperature monitoring, e.g. in hyperthermia for cancer treatment.

Existing methods include invasive methods such as rectal probes, gastro-intestinal sensors, surgically inserted thermometers, etc. Ingestible sensors are short-range wireless devices which measure the temperature somewhere in the digestive track for a limited time while the device is in the body. Magnetic Resonance Imaging (MRI) can be used for measuring temperature distribution with high spatial resolution, but is very expensive and not portable. With current trends to personalize medicine with wearable wireless sensors, there is a need for continuous temperature monitoring devices placed on different parts of the body. There has been limited research in microwave core-body thermometry, mainly limited to infant brain temperature measurements (e.g. [3,4]), for monitoring astronaut temperature in space-suits [5], and for abnormal bladder functions [6]. In these cases typically the environment is shielded or relatively large shielded probes are used, resulting in non-wearable devices.

In this paper, we present a 1.4GHz microwave radiometer that is capable of measuring the sub-surface temperature of a water phantom at a depth up to 4cm. A block diagram of the microwave thermometer is shown in Fig.1.
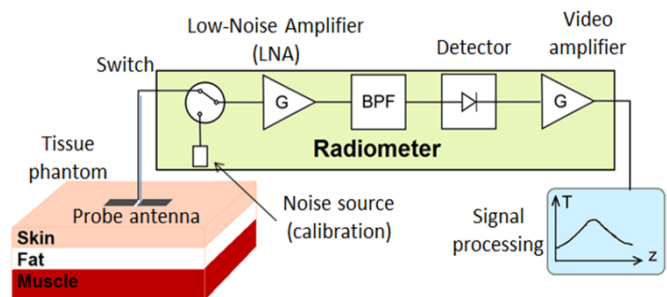

Fig. 1. A probe antenna is placed on the skin and couples received power to a Dicke radiometer. The probe receives total black-body power from all tissue layers, and some from outside the body. An inverse problem needs to be solved to determine the temperature corresponding to different tissue layers.

The remainder of this paper describes the probe and radiometer implementation, as well as calibration and the method used to estimate the temperature at some depth, given the measurement of total black-body power. Two probe designs are compared, and the radiometer is designed based on inexpensive commercially-available components. The 1.4GHz frequency of operation is chosen for deep penetration into tissues. The narrow bandwidth of about 20MHz around 1.4GHz is chosen for low RFI, since 1.4GHz is a quiet band reserved for radio-astronomy and therefore has less man-made interference.

II. RADIOMETER DESIGN AND IMPLEMENTATION

The radiometer device from Figure 1 can be implemented in a variety of architectures, such as the ones used in radio-astronomy [7], terrestrial remote sensing, fire-monitoring, etc. In most of these applications, the object is in the far field of an antenna receiving plane waves radiated by the object. In the core body thermometry case, however, the power radiated by the different tissue layers is received by a probe situated in the near field, on the skin.

In a narrow measurement frequency bandwidth (B), the power received can be approximated by the simple thermal (white) noise expression $P=kT_AB$, where T_A is the antenna temperature which depends on both the physical temperature and the antenna directional parameter, which describes the power an antenna receives from a cone described by spherical angles (θ, ϕ). Once the power is measured by the radiometer, a model is needed for the tissue stack-up to determine the temperature distribution. This has been done with near-field weighting functions estimated from some type of electromagnetic simulation (e.g. FDTD, FEM, semi-analytical [8]). Referring to Fig.2, the antenna temperature is expressed as a weighted average of the temperature of the tissue layers:

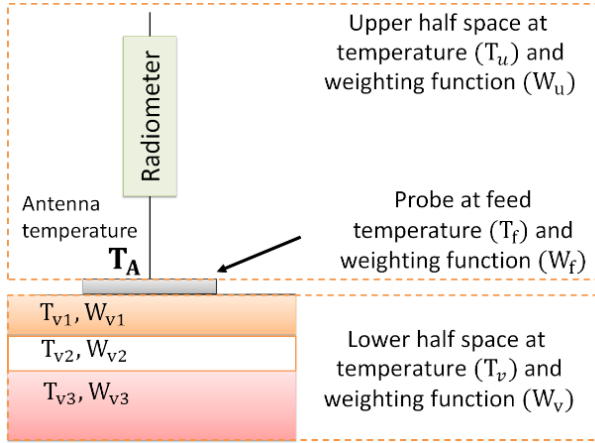$$T_A = T_uW_u + T_fW_f + T_{v1}W_{v1} + T_{v2}W_{v2} + T_{v3}W_{v3} \qquad (1)$$

Fig. 2. Antenna temperature (TA) is a weighted average of the temperature of the different tissue layers, and weighting functions (W) are used to define the antenna temperature.

To measure the total power, and therefore T_A which can then be used to back out the layer temperatures, we implemented a radiometer described below. The square-law diode detector in Fig.1 is a Skyworks Schottky diode SMS7630-079 and is matched with a lumped element LC match (C=4.7pF, L=15nH). The measured responsivity of the square-law detector is shown in Fig.3 and is seen to be 25mV/μW at 1.4GHz. The detector is matched best at 1.4 GHz when driven with an RF input power of -40 dBm.
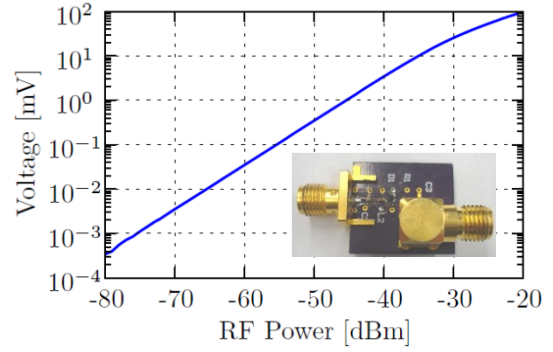

Fig.3. Measured responsivity of the diode detector at 1.4GHz, with a photograph of the implemented circuit shown in inset.

The next step in the receiver design is to determine the necessary gain and receiver sensitivity requirements. The RF power is calculated using a 27-MHz bandwidth and normal body temperature ($T≈310$ K) to be P_{RFin} = -99.4 dBm. If the desired output voltage is 100μV, which places the input power within the square-law region of the detector, a minimum gain of 45dB is required. The radiometric resolution is written as:

$$\Delta T = \frac{T_A + T_{rec}}{\sqrt{B\tau}} \qquad (2)$$

where T_A is the antenna temperature including the ohmic losses, T_{rec} is the receiver temperature. For a resolution of ΔT = 0.2K, to determine the required receiver temperature we assumed the integration time to be τ = 0.333s. The corresponding noise figure is NF =3dB. With this information, parts are selected that achieve the appropriate gain and cascaded noise figure, as detailed in Fig.4. The switch in the block diagram of Fig.4 is required to calibrate the radiometer. T_h and T_c are hot and cold calibration standards, in this case an Agilent 346A noise source and a matched load at room temperature, respectively. An output voltage of 127.6 μV for an input power of -100 dBm was measured and the measured frequency response of the radiometer is shown in Figure 5.
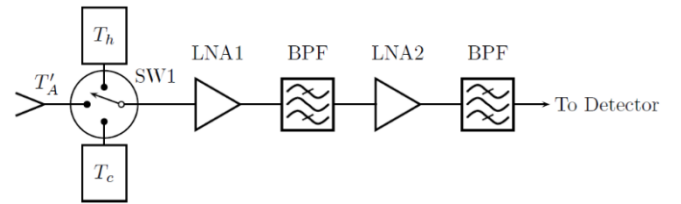
COMPONENTS FOR 1.4GHZ RADIOMETER

Element	Manufacturer	Part Number	G[dB]	NF[dB]
SW1	Hittite	HMC345LP3	-2	2
LNA1	Mini-Circuits	RAMP-33LN	16.7	1
BPF	Mini-Circuits	VBFZ-1400	-2	2
LNA2	Mini-Circuits	TAMP	34.9	0.6

Fig. 4. Block diagram of the 1.4 GHz radiometer along with the element names, part numbers, gains and noise figures.
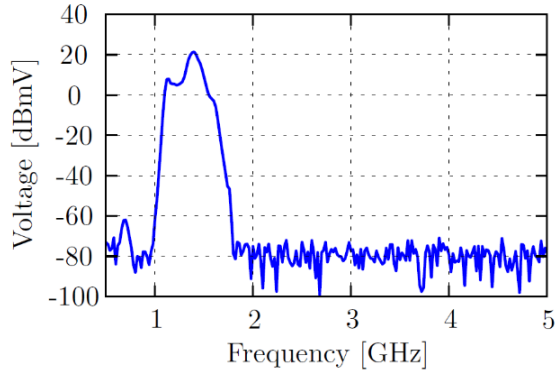
Fig. 5. Measured voltage relative to 1mV of the 1.4GHz receiver vs. RF input over frequency at an input power of -80 dBm.

Fig. 7. Photograph of measurement setup with 1.4GHz folded dipole probe placed on the surface of the water phantom.

III. PROBES AND SYSTEM MEASUREMENTS

Two different probes are designed for operation in the quiet 1.4GHz band: a folded dipole and a circular patch, Fig.6. the patch is backed by a ground plane and is narrowband, while the dipole has wider bandwidth and is less shielded from the air side. The dipole is fed by a tapered balun and fabricated on Rogers 4350B (ε_r=3.66). The return loss is greater than 20 dB in the band of interest [9]. The patch is fabricated on a Rogers 6010 (ε_r=10.2) substrate with a superstrate of the same material. The superstrate reduces the sensitivity of the probe to the surrounding media, which is advantageous for complex and variable tissue thicknesses in human bodies. The narrower bandwidth of the patch helps reduce RFI. The measured return loss is better than 20 dB in the frequency band of interest.
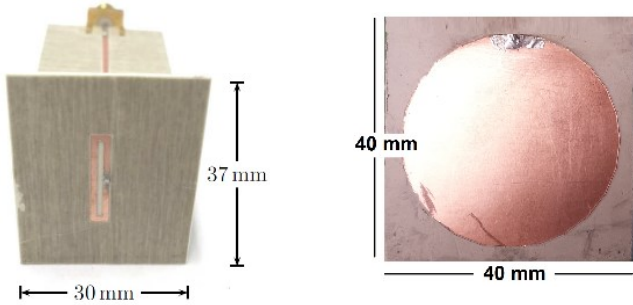

Fig. 6. Two probes used for measurements at 1.4GHz: a printed folded dipole with a balun feed (left) and a circular patch used with a high-permittivity superstrate (right).

The two planar compact probe antennas are positioned on the surface of a half-space water phantom. The test setup, shown in Fig.7, is placed in an anechoic chamber to eliminate unknown interference. A hot and cold noise source calibration is performed. The temperature of the load is measured with a thermocouple connected to a PicoTech.0 TC-08 data logger. The calibration is performed every second with an equal dwell time on each of the standards and the probe.
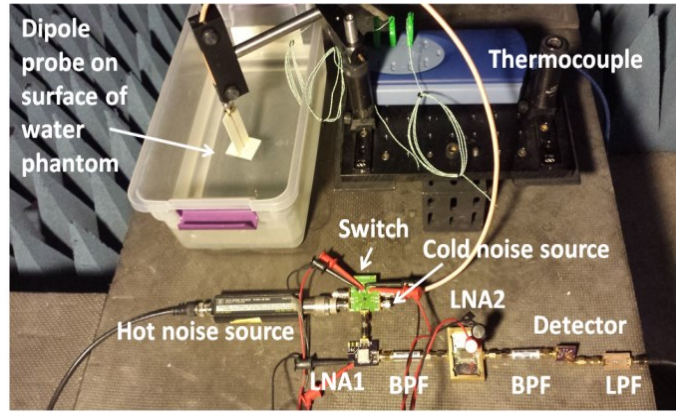
The received data at the output of the detector, which is related to the unknown temperature measured by the probe, is then processed using Eq.(1). A thermocouple sensor is placed in the water bath, which is heated to 40°C when the patch is used, and to 35°C when the dipole probe is used. The measured data in Fig. 8 compares the thermocouple measurements with passive radiometric measurements using the two probes. The estimated temperature from both probes follows the thermocouple measurement within 0.5K as the water phantom cools to below 30°C in 55min. In each case, a fixed bias of a few degrees in the data is calibrated out, and the bias is larger for the patch probe .
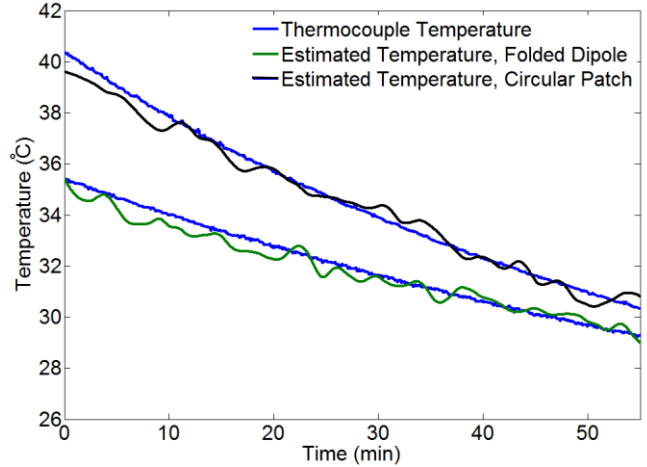

Fig. 8. Calibrated radiometric estimate of the temperature of a water half-space using the 1.4 GHz radiometer compared to thermocouple measurement. The water phantom is heated to 40°C for the patch probe data, and to 35°C for the dipole case, and measurements were taken as the water cooled until reaching 30°C.

IV. CONCLUSION

We present two different planar compact probe antennas and a radiometer assembled from off-the-shelf components for measuring sub-surface temperature with a 0.5K accuracy. Ongoing research is focused on subsurface temperature

measurements on a three-layer phantom that mimics skin, fat and muscle, as in e.g. [9]. Preliminary data shows similar accuracy as the data in Fig.8, but in this case the estimation algorithm is more complicated. Several algorithms are being investigated currently: least-squared method with 1 and 2 unknowns, and optimal estimation with 1 and 2 unknowns. It appears that optimal estimation with 2 unknowns gives the smallest error, followed by the least-squared method with 1 unknown. The estimation includes determination of the weighting functions from Eq. (1).

A considerable challenge in measuring black-body radiation far from the peak of the Boltzmann curve are the low power levels accompanied by high levels of man-made interference in the radio spectrum. For this reason, we have chosen to trade integration time (on the order of seconds) with narrow bandwidth. The filters used in the prototype from Fig.7 do not have adequately narrow passbands, and SAW filters could improve this performance. Finally, much of the interference is due to the hybrid nature of this initial prototype, which consists of several boards connected externally, with the final assembly acting as a receiving antenna. Miniaturization by integration of the radiometer in a GaAs MMIC (switch, LNA and noise source), and CMOS readout circuit, could provide significant improvements and is the topic of future research. For example, a GaAs cold noise source chip has already been designed and measured [10], and can replace large commercial noise sources.

REFERENCES

[1] K. Kräuchi *et al.*,"Functional link between distal vasodilation and sleep-onset latency" *American Journal of Physiology - Regulatory, Integrative and Comparative Physiology*, vol. 278, pp. R741–R748, 2000. 129-131, 140

[2] K. Kräuchi, "How is the circadian rhythm of core body temperature regulated?" *Clin. Auton. Res.* 2002;12:147–9.

[3] J. W. Hand *et al.*, "Monitoring of deep brain temperature in infants using multi-frequency microwave radiometry and thermal modelling," *Physics in Medicine and Biology*, vol. 46, no. 7, p. 1885, 2001.

[4] S. Jacobsen and P. Stauffer, "Multifrequency radiometric determination of temperature profiles in a lossy homogeneous phantom using a dual-mode antenna with integral water bolus," *IEEE Trans. Microw. Theory Techn.* pp. 1737–1746, Jul. 2002.

[5] Q. Bonds *et al.*, "Towards core body temperature measurement via close proximity radiometric sensing," *Sensors Journal, IEEE*, no. 99, p. 1, 2011.

[6] Klemetsen, Ø. et al. "Design of medical radiometer front-end for improved performance," *Progress in electromagnetics research B. Pier B* 27 (2011): 289–306

[7] J. D. Kraus, *Radio Astronomy*, 2nd ed. Cygnus-Quasar Books, 1976, pp. 1-3, 20-23, 66

[8] R.Scheeler *et al.*, "Sensing Depth of Microwave Radiation for Internal Body Temperature Measurement", *IEEE Trans. Antennas Prop.*, Vol. 62, No. 3, March 2014.

[9] R.Scheeler *et al.*, "Microwave Radiometry for Internal Body Temperature Monitoring"*IEEE EMBC'14*, Chicago, Aug. 2014.

[10] R. Scheeler, Z. Popović, "A 1.4GHz MMIC Active Cold Noise Source," *IEEE Compound Semiconductor IC Symposium*, October 13-16, 2013, Monterey, CA.